

Published in final edited form as:

Bioorg Med Chem Lett. 2009 May 15; 19(10): 2865–2869. doi:10.1016/j.bmcl.2009.03.080.

Benzothiophene piperazine and piperidine urea inhibitors of fatty acid amide hydrolase (FAAH)

Douglas S. Johnson^{a,b,§}, Kay Ahn^{a,b}, Suzanne Kesten^a, Scott E. Lazerwith^a, Yuntao Song^a, Mark Morris^a, Lorraine Fay^a, Tracy Gregory^{a,b}, Cory Stiff^{a,b}, James B. Dunbar Jr.^a, Marya Liimatta^{a,c}, David Beidler^{a,d}, Sarah Smith^{a,d}, Tyzoon K. Nomanbhoy^e, and Benjamin F. Cravatt^f

^aPfizer Global Research and Development, 2800 Plymouth Road, Ann Arbor, MI 48105, USA

^bPfizer Global Research and Development, Eastern Point Road, Groton, CT 06340, USA

^cPfizer Global Research and Development, 620 Memorial Drive, Cambridge, MA 02139, USA

^dPfizer Global Research and Development, 700 Chesterfield Parkway, Chesterfield, MO 63017, USA

^eActivX Biosciences, 11025 North Torrey Pines Road, La Jolla, CA 92037, USA

^fDepartment of Chemical Physiology, The Skaggs Institute for Chemical Biology, The Scripps Research Institute, 10550 North Torrey Pines Road, La Jolla, CA 92037, USA

Abstract

The synthesis and structure–activity relationships (SAR) of a series of benzothiophene piperazine and piperidine urea FAAH inhibitors is described. These compounds inhibit FAAH by covalently modifying the enzyme’s active site serine nucleophile. Activity-based protein profiling (ABPP) revealed that these urea inhibitors were completely selective for FAAH relative to other mammalian serine hydrolases. Several compounds showed *in vivo* activity in a rat complete Freund’s adjuvant (CFA) model of inflammatory pain.

Keywords

FAAH inhibitor; Fatty acid amide hydrolase; Urea; Activity-based protein profiling; Covalent inhibitor

Fatty acid amide hydrolase (FAAH) is an integral membrane enzyme that degrades the fatty acid amide family of signaling lipids, including the endocannabinoid anandamide.¹ Genetic^{1g} or pharmacological^{1f} inactivation of FAAH leads to elevated endogenous levels of fatty acid amides and a range of behavioral effects including analgesic and anti-inflammatory phenotypes in rodents. Importantly, these behavioral phenotypes occur in the absence of alterations in motility, weight gain, or body temperature that are typically observed with direct cannabinoid receptor 1 (CB1) agonists, indicating that FAAH may represent an attractive therapeutic target for the treatment of inflammatory pain and related conditions.² Several classes of FAAH inhibitors have been reported including electrophilic ketones (e.g., OL-135³), carbamates (e.g., URB597⁴ and SA-47⁵) and, more recently, piperidine/piperazine ureas (e.g., PF-750⁶ and Takeda-25/JNJ-1661010⁷) (Fig. 1). We recently reported that PF-750 inhibits FAAH by covalently modifying the enzyme’s active site serine

[§]corresponding author: doug.johnson@pfizer.com.

nucleophile and is completely selective for FAAH relative to other mammalian serinehydrolases.^{6a} In this Letter, we describe the synthesis and structure–activity relationships (SAR) of a series of benzothiophene piperazine and piperidine urea FAAH inhibitors.

A series of piperazine phenyl ureas, exemplified by **1**, was discovered by high throughput screening of the Pfizer chemical file against human FAAH (Fig. 2). We prepared piperazine phenyl urea intermediate **2** and performed a series of reductive aminations with various aromatic aldehydes (Scheme 1, **Eqs. 1** and **2**). This allowed us to easily vary the aldehyde component and resulted in the identification of several bicyclic cores including PF-622^{6a} and a series of benzothiophenes represented by **4h**, which is the subject of this manuscript (Scheme 1, **Eq. 2**).

We then explored the benzothiophene lead **4h** in more detail. Therefore, the benzothiophene piperazine intermediate **5** was prepared according to **Equation 3** and reacted with various commercially available alkyl and aryl isocyanates or phenyl carbamates of heterocyclic amines⁸ to give the corresponding piperazine ureas **4** and **6** (Scheme 1).

Scheme 2 and Scheme 3 outline the synthesis of representative piperidine urea FAAH inhibitors utilized in the current studies. Lithiation of benzothiophene **7** followed by reaction with Weinreb amide **8** provided ketone **9** in good yield.⁹ Ketone **9** was reduced with sodium borohydride to give alcohol **10** which underwent elimination when treated with *p*-toluene sulfonic acid (TsOH). The resulting double bond was hydrogenated to give piperidine **11** which was treated with isocyanate **12** as described previously to give the desired urea **13**.⁸

The linker analogs **15–18** were synthesized according to Scheme 3. Deprotection of Boc-piperidine **14** with TFA followed by reaction with isocyanate **12** afforded urea **15** with a ketone linker. Wittig olefination of ketone **15** provided compound **16** with a methylene substituted linker. Hydrogenation of the double bond gave **17** with a methyl substituted linker as the racemate and the enantiomers were separated by chiral chromatography. Furthermore, ketone **15** was reduced to give racemic **18** with a hydroxy substituted linker.

As previously reported, these piperidine/piperazine ureas inhibit FAAH by covalent carbamylation of the catalytic Ser241 nucleophile.^{6a,6b} Therefore, the potency of these benzothiophene piperidine/piperazine urea inhibitors were determined by the second order rate constants k_{inact}/K_i values using an enzyme-coupled FAAH assay as described previously.^{6b,10} Unlike IC_{50} values, k_{inact}/K_i values do not change with various preincubation times and have been described as the best measure of potency for irreversible inhibitors.¹¹

Table 1 shows the SAR of the right hand portion of the urea. The alkyl ureas (**4a–g**) had very low potency for FAAH, which is similar to what has been observed for *N*-alkylurea analogs of URB597.^{4a} In contrast, we found that aryl ureas such as phenyl urea **4h** were potent FAAH inhibitors. Next, we investigated a series of heteroaromatic ureas (**4i–l**, **6a**) in part to avoid the generation of aniline upon covalent binding to FAAH. The 3-aminopyridyl group (**6a**) was preferred over the 2-aminopyridyl (**4i**) and 3-aminopyridazinyl (**4j**) groups in the benzothiophene series. The SAR of the heterocyclic group was highly sensitive. For example, isoxazole **4k** retained potency, while the potency was lost with methylthiazole **4l**, which is consistent with observations made by Keith et al. in a related thiadiazolopiperazinyl urea series.^{7b} Boger and co-workers also observed that subtle changes in the central heterocycle of α -ketoheterocycle FAAH inhibitors greatly influence inhibitor activity.^{3c} Also it is interesting to note that isoxazole **4k** exhibited equal potency for hFAAH and rFAAH, while phenyl urea **4h** and pyridazine urea **4j** showed higher potency for hFAAH than rFAAH.

Next, we investigated the effect of substituents at the 6-position of the 3-amino pyridine (Table 2). The compounds with 6-methoxy (**6g**), 6-amino (**6i**) and 6-NHAc (**6n**) substituents are roughly equipotent to **6a**, while the 6-Cl (**6d**) and 6-NHMe (**6j**) groups result in compounds that are about twofold less potent and the potency is further diminished by the 6-NHEt (**6l**) substituent (fourfold less potent than **6a**). Furthermore, 6-CF₃ (**6c**) and 6-NEt₂ (**6m**) substituents are detrimental to activity. Taken together with the results in Table 1, it is clear that the nature of the aromatic amine portion of the urea is critical for activity, but the potency does not appear to correlate with the leaving group ability. There appears to be a steric limitation at the 6-position as hFAAH potency generally decreases with the larger substituents (i.e., $h k_{\text{inact}}/K_i$ for NH₂ > NHMe > NMe₂ > NEt₂). Interestingly, several 6-amino compounds (**6j–m**) actually show a preference for rFAAH over hFAAH.

Subsequent SAR studies focused on optimization of the benzothiophene substitution while maintaining the optimal 3-aminopyridyl urea (Table 3). It was found that incorporating an alkyl group at the 3-position of the benzothiophene (R¹) led to improved potency. For example, compound **6a** was 3–4-fold more potent than the unsubstituted benzothiophene **19**. In most cases for hFAAH, the piperidine analogs were slightly more potent than the corresponding piperazine analogs (i.e., **20** > **6a**), which is most likely a result of more favorable Van der Waals interactions of the piperidine with the acyl chain binding channel of FAAH.^{1b,6b} Substitution was tolerated at the 4- and 5-position of the benzothiophene (**24–36**), but no significant improvement in potency was realized. Conversely, moving the substituent (R⁴) to the 6-position of the benzothiophene impaired potency (**37–39**), which is predicted to introduce steric clashes with the FAAH protein (Fig. 5).

As shown in Table 4, the potency is maintained when a ketone or methylene is incorporated within the linker (**15** and **16**, Scheme 3) whereas the reduced compounds **17** and **18** with methyl and hydroxyl substituents lose much of their activity. The sp² hybridization of the ketone and methylene linker compounds **15** and **16** imposes a conformational constraint that appears to help position the benzothiophene in a more favorable binding orientation. The SAR in this linker region is sensitive as further evidenced by the >10-fold difference in potency for the enantiomers of **17**.

We have proposed that the urea may be activated upon binding in the active site of FAAH by undergoing a conformational change that diminishes conjugation of the nitrogen lone pair with the carbonyl, which would activate the urea toward nucleophile attack as shown in Figure 3.^{6a} It appears that a cyclic secondary amine such as piperazine or piperidine is critical for activation of the urea as ureas prepared from primary amines are ineffective.^{4a}

Compound **13** (Fig. 4) and compound **38** (Fig. 5) were modeled,¹² using Sybyl 8.0, into the ‘humanized’ rat FAAH (h/rFAAH) crystal structure (2VYA).^{6b} Compound **13** fit within the binding site in almost identical fashion to that of PF-750 with only very slight movement of the surrounding residue atoms, in essence, occupying virtually identical space. The green surface depicting the binding site volume and the space-filled representations were generated from the compound **13**-h/rFAAH model and are virtually identical to those generated from the PF-750-h/rFAAH crystal structure. In contrast, when the model of compound **38**-h/rFAAH was minimized, there was a significant shift in the position of the side chain of Met436. As shown in Figure 5, the ethoxy portion of compound **38** extends beyond the green surface generated from the compound **13** model illustrating the increased size of the ligand and the subsequent displacement (i.e., push) of the Met436 side chain. This steric interaction with Met436 could explain the decreased potency of compound **38**.

To assess the selectivity of the benzothiophene piperidine/piperazine urea series, compounds **6b**, **6g** (PF-465), and **13** (PF-946) were profiled at 100 μM by competitive activity-based

protein profiling (ABPP)¹³ in a number of different proteomes derived from mouse and human sources (Fig. 6). Competitive ABPP provides a global view of the proteome-wide selectivity of enzyme inhibitors as described previously.^{13b,13c} In the case of FAAH inhibitors, we used a reporter-tagged fluorophosphonate (FP) ABPP probe,^{13c} which serves as a general activity-based profiling tool for the serine hydrolase super family.^{13d,13e} Serine hydrolases that show significant reductions in FP probe labeling intensity in the presence of inhibitor are scored as targets of the compound. The selectivity of compounds **6b**, **6g**, and **13** was compared to that of URB597, which was profiled at 10 and 100 μM . Gel images of soluble proteomes of mouse liver, mouse kidney, human liver, and human heart and the membrane proteome of human brain are shown in Figure 6. Consistent with previous reports,^{6a,14} multiple off-targets were observed in peripheral tissues for URB597 even at 10 μM , particularly amongst FP-labeled proteins migrating between 55 and 65 kDa. It is noteworthy that URB597, which has been shown to be highly selective for serine hydrolases in mouse brain proteomes, inhibits at least one additional hydrolase migrating at 55–60 kDa in the human brain membrane proteome. In contrast, no off-targets were observed for compounds **6b**, **6g**, and **13** even when tested at 100 μM (Fig. 6). Under the assay conditions, compounds **6b**, **6g**, **13**, and URB597 completely inhibited FAAH from both mouse and human tissues.

Next we selected compound **6g** (PF-465) to assess its *in vivo* efficacy in a rat model of inflammatory pain. Subcutaneous injection of complete Freund's adjuvant (CFA) into the plantar surface of the hind paw produced a significant decrease in mechanical paw weight threshold (PWT) at 5 days post injection (Fig. 7). Compound **6g** dosed at 3, 10 and 30 mg/kg (ip) caused a dose-dependent inhibition of mechanical allodynia with a minimum effective dose (MED) of 10 mg/kg. At doses of 10 and 30 mg/kg, compound **6g** inhibited pain responses to an equivalent degree as the nonsteroidal anti-inflammatory drug naproxen (10 mg/kg, ip).

In conclusion, we have described a series of benzothiophene piperazine/piperidine urea FAAH inhibitors that covalently modify the enzyme's active site serinenucleophile. Activity-based protein profiling revealed that these urea inhibitors are highly selective for FAAH relative to other mammalian serine hydrolases. Furthermore, *in vivo* activity was demonstrated in a rat CFA model of inflammatory pain. Additional SAR development of this class of piperazine/piperidine urea FAAH inhibitors will be reported in due course.

References and notes

- (a) Cravatt BF, Giang DK, Mayfield SP, Boger DL, Lerner RA, Gilula NB. *Nature*. 1996; 384:83. [PubMed: 8900284] (b) Bracey MA, Hanson MA, Masuda KR, Stevens RC, Cravatt BF. *Science*. 2002; 298:1793. [PubMed: 12459591] (c) Cravatt BF, Lichtman AH. *Curr. Opin. Chem. Biol.* 2003; 7:469. [PubMed: 12941421] (d) McKinney MK, Cravatt BF. *Annu. Rev. Biochem.* 2005; 74:411. [PubMed: 15952893] (e) Ahn K, McKinney MK, Cravatt BF. *Chem. Rev.* 2008; 108:1687. [PubMed: 18429637] (f) Cravatt BF, Demarest K, Patricelli MP, Bracey MH, Giang DK, Martin BR, Lichtman AH. *Proc. Natl. Acad. Sci. U.S.A.* 2001; 98:9371. [PubMed: 11470906] (g) Kathuria S, Gaetani S, Fegley D, Valino F, Duranti A, Tontini A, Mor M, Tarzia G, La Rana G, Calignano A, Giustino A, Tattoli M, Palmery M, Cuomo V, Piomelli D. *Nat. Med.* 2003; 9:76. [PubMed: 12461523]
- (a) Lambert DM, Fowler CJ. *J. Med. Chem.* 2005; 48:5059. [PubMed: 16078824] (b) Pacher P, Batkai S, Kunos G. *Pharmacol. Rev.* 2006; 58:389. [PubMed: 16968947] (c) Di Marzo V. *Nat. Rev. Drug Disc.* 2008; 7:438. (d) Seierstad M, Breitenbucher JG. *J. Med. Chem.* 2008; 51:7327. [PubMed: 18983142]
- (a) Boger DL, Sato H, Lerner AE, Hedrick MP, Fecik RA, Miyauchi H, Wilkie GD, Austin BJ, Patricelli MP, Cravatt BF. *Proc. Natl. Acad. Sci. U.S.A.* 2000; 97:5044. [PubMed: 10805767] (b) Boger DL, Miyauchi H, Du W, Hardouin C, Fecik RA, Cheng H, Hwang I, Hedrick MP, Leung D,

- Acevedo O, Guimaraes CRW, Jorgensen WL, Cravatt BF. *J. Med. Chem.* 2005; 48:1849. [PubMed: 15771430] (c) Garfinkle J, Ezzili C, Rayl TJ, Hochstatter DG, Hwang I, Boger DL. *J. Med. Chem.* 2008; 51:4392. [PubMed: 18630870]
4. (a) Tarzia G, Duranti A, Tontini A, Piersanti G, Mor M, Rivara S, Plazzi PV, Park C, Kathuria S, Piomelli D. *J. Med. Chem.* 2003; 46:2352. [PubMed: 12773040] (b) Mor M, Rivara S, Lodola A, Plazzi PV, Tarzia G, Duranti A, Tontini A, Piersanti G, Kathuria S, Piomelli D. *J. Med. Chem.* 2004; 47:4998. [PubMed: 15456244] (c) Tarzia G, Duranti A, Gatti G, Piersanti G, Tontini A, Rivara S, Lodola A, Plazzi PV, Mor M, Kathuria S, Piomelli D. *Chem. Med. Chem.* 2006; 1:2352.
 5. Abouab-Dellah, A.; Burnier, P.; Hoornaert, C.; Jeunesse, J.; Puech, F. Patent. WO 2004/099176. 2004. US 2006/0089344, 2006.
 6. (a) Ahn K, Johnson DS, Fitzgerald LR, Liimatta M, Arendse A, Stevenson T, Lund ET, Nugent RA, Nomanbhoy TK, Alexander JP, Cravatt BF. *Biochemistry.* 2007; 46:13019. [PubMed: 17949010] (b) Mileni M, Johnson DS, Wang Z, Everdeen D, Liimatta M, Pabst B, Bhattacharya K, Nugent RA, Kamtekar S, Cravatt BF, Ahn K, Stevens RC. *Proc. Natl. Acad. Sci. U.S.A.* 2008; 105:12820. [PubMed: 18753625] (c) Apodaca, R.; Breitenbucher, JG.; Pattabiraman, K.; Seierstad, M.; Xiao, W. Patent. WO 2006/074025. 2006.
 7. (a) Matsumoto, T.; Kori, M.; Miyazaki, J.; Kiyota, Y. Patent. WO 2006/054652. 2006. EP 1813606, 2007. (b) Keith JM, Apodaca R, Xiao W, Seierstad M, Pattabiraman K, Wu J, Webb M, Karbarz MJ, Brown S, Wilson S, Scott B, Tham C-S, Luo L, Palmer J, Wennerholm M, Chaplan S, Breitenbucher JG. *Bioorg. Med. Chem. Lett.* 2008; 18:4838. [PubMed: 18693015] (c) Karbarz MJ, Luo L, Chang L, Tham C-S, Palmer JA, Wilson SJ, Wennerholm ML, Brown SM, Scott BP, Apodaca RL, Keith JM, Wu J, Breitenbucher JG, Chaplan SR, Webb M. *Anesthesia Analgesia.* 2009; 108:316. [PubMed: 19095868]
 8. (a) Thavonekham B. *Synthesis.* 1997:1189. (b) Swanson DM, Dubin AE, Shah C, Nasser N, Chang L, Dax SL, Jetter M, Breitenbucher JG, Liu C, Mazur C, Lord B, Gonzales L, Hoey K, Rizzolio M, Bogenstaetter M, Codd EE, Lee DH, Zhang S-P, Chaplan SR, Carruthers NI. *J. Med. Chem.* 2005; 48:1857. [PubMed: 15771431]
 9. Matsunaga N, Kaku T, Itoh F, Tanaka T, Hara T, Miki H, Iwasaki M, Aono T, Yamaoka M, Kusaka M, Tasaka A. *Bioorg. Med. Chem.* 2004; 12:2251. [PubMed: 15080924]
 10. Ahn, K. Patent. WO 2006/085196. 2006.
 11. Copeland, RA. *Enzymes: A Practical Introduction to Structure, Mechanism, and Data Analysis.* 2nd ed.. New York: Wiley-VCH; 2000. p. 318-349.
 12. All the hydrogens were added to the protein and each compound was covalently attached to the sidechain oxygen of Ser241. The protein/ligand structures were then minimized using the Sybyl forcefield with the backbone atoms held constant; charges were not used. These minimized structures were then compared to the PF-750-h/rFAAH crystal structure.
 13. (a) Cravatt BF, Wright AT, Kozarich JW. *Annu. Rev. Biochem.* 2008; 77:383. [PubMed: 18366325] (b) Kidd D, Liu Y, Cravatt BF. *Biochemistry.* 2001; 40:4005. [PubMed: 11300781] (c) Leung D, Hardouin C, Boger DL, Cravatt BF. *Nat. Biotechnol.* 2003; 21:687. [PubMed: 12740587] (d) Patricelli MP, Giang DK, Stamp LM, Burbaum JJ. *Proteomics.* 2001; 1:1067. [PubMed: 11990500] (e) Liu Y, Patricelli MP, Cravatt BF. *Proc. Natl. Acad. Sci. U.S.A.* 1999; 96:14694. [PubMed: 10611275]
 14. (a) Alexander JP, Cravatt BF. *Chem. Biol.* 2005; 12:1179. [PubMed: 16298297] (b) Zhang D, Saraf A, Kolasa T, Bhatia P, Zheng GZ, Patel M, Lannoye GS, Richardson P, Stewart A, Rogers JC, Brioni JD, Surowy CS. *Neuropharmacol.* 2007; 52:1095.
 15. The hFAAH (amino acids 32–579) and rFAAH (amino acids 30–579) constructs were generated as the N-terminal transmembrane-deleted truncated forms with N-terminal His₆ tags, and were expressed in *E. coli* and purified as previously described.^{6b} Both hFAAH and rFAAH enzymes used in the present study had purity greater than 95% based on SDS–PAGE visualized by Coomassie blue staining. The GDH-coupled FAAH assay was performed for determination of potencies (k_{inact}/K_i values) of inhibitors in 384-well microplates with a final volume of 50 μL . The details on the assay and derivations of the overall potency, k_{inact}/K_i value, have been described previously.^{6b} In the 384-well format assay, the k_{inact}/K_i values were generally calculated from the slope, $k_{\text{inact}}/[K_i(1 + [S]/K_m)]$, which is obtained from the k_{obs} versus $[I]$ linear lines. The k_{inact}/K_i values are averages of at least two independent experiments.

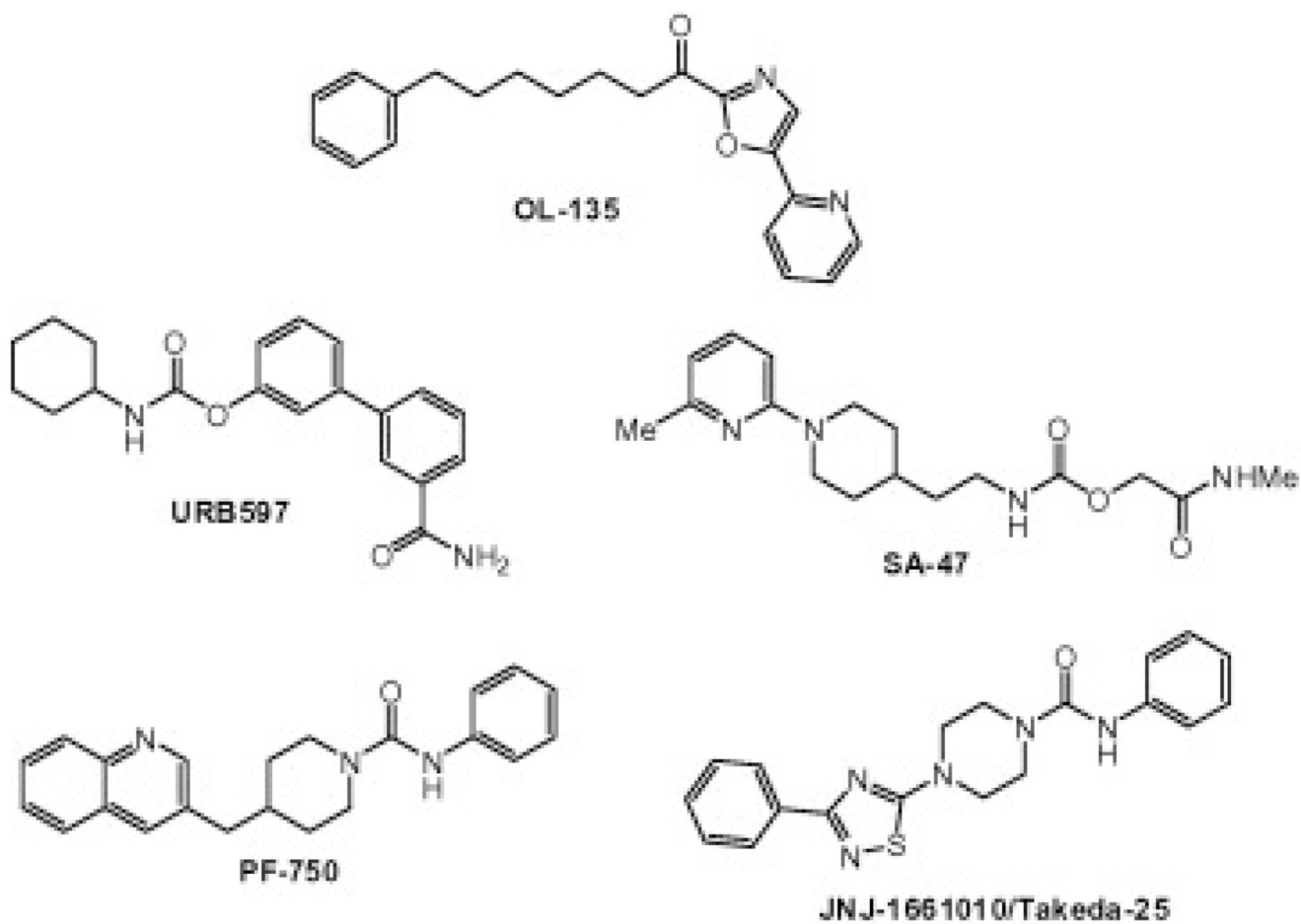


Figure 1.
Structures of FAAH inhibitors.

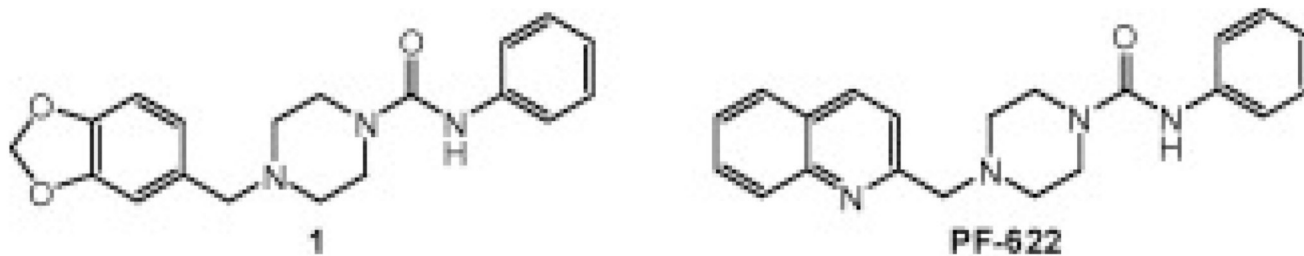


Figure 2.
Structures of HTS lead (1) and PF-622.

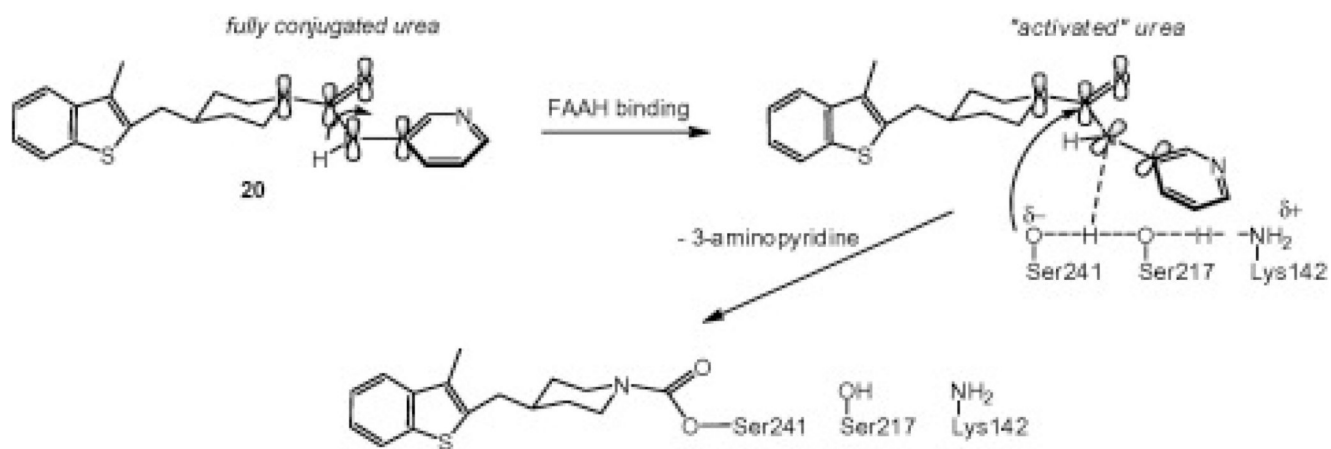


Figure 3. Proposed mechanism of covalent inhibition of FAAH by piperidine ureas. The catalytic triad Ser-Ser-Lys is shown.

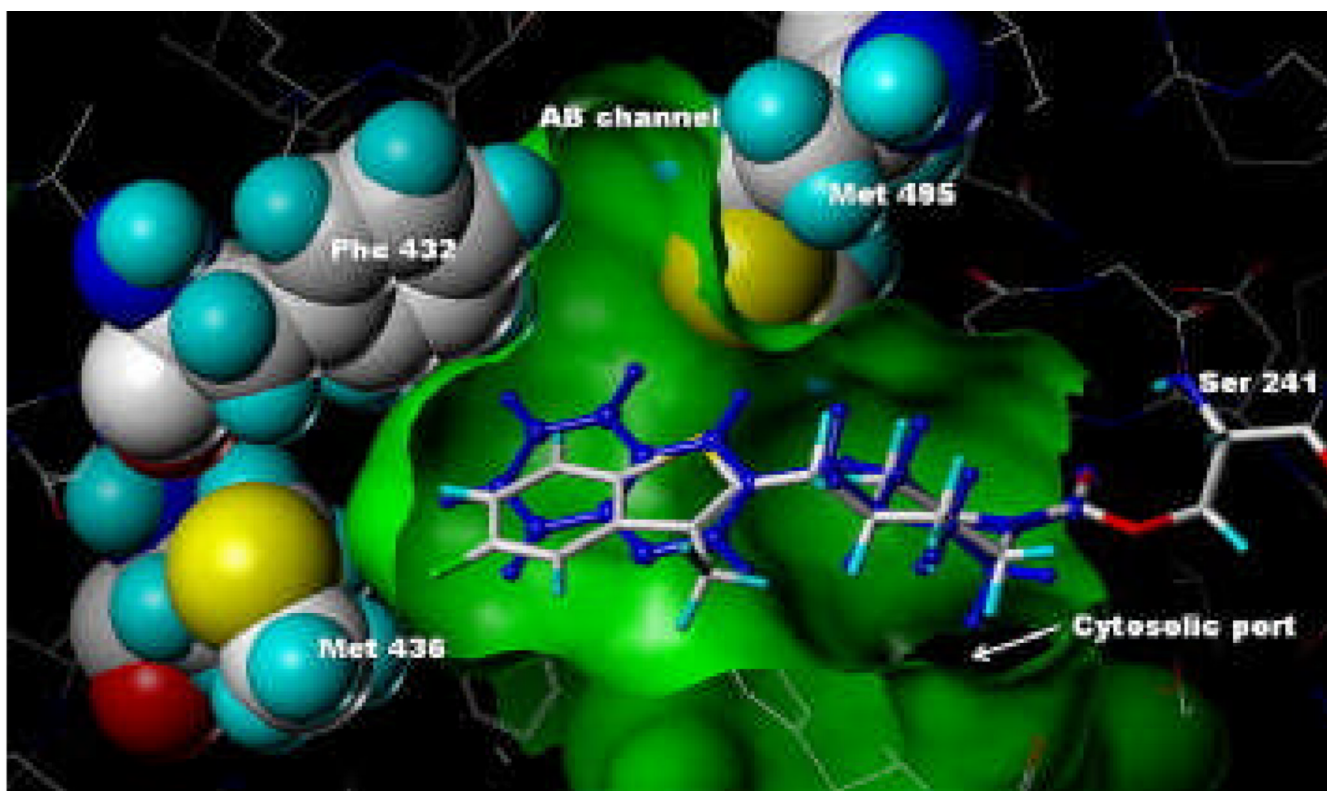


Figure 4. Model of compound **13** covalently attached to Ser241 of h/rFAAH using coordinates from the PF-750-h/rFAAH crystal structure.^{6b} Overlay with PF-750 shown in blue.

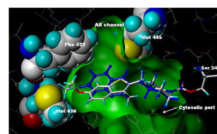


Figure 5. Model of compound **38** covalently attached to Ser241 of h/rFAAH using coordinates from the PF-750-h/rFAAH crystal structure.^{6b} Overlay with PF-750 shown in blue.

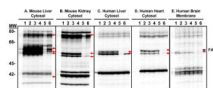


Figure 6. Selectivity profiling of FAAH inhibitors. Gel images of proteomes labeled with FP-rhodamine in the absence or presence of FAAH inhibitors (Lane 1, buffer; lane 2, **6b** at 100 μM ; lane 3, **6g** at 100 μM ; lane 4, **13** at 100 μM ; lane 5, URB597 at 100 μM ; lane 6, URB597 at 10 μM). Inhibited bands are shown with arrows. (A) soluble mouse liver proteome, (B) soluble mouse kidney proteome, (C) soluble human liver proteome, (D) soluble human heart proteome, and (E) human brain membrane proteome. Fluorescent gel signals shown in grayscale.

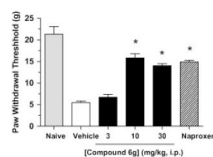
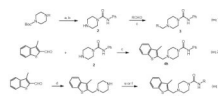
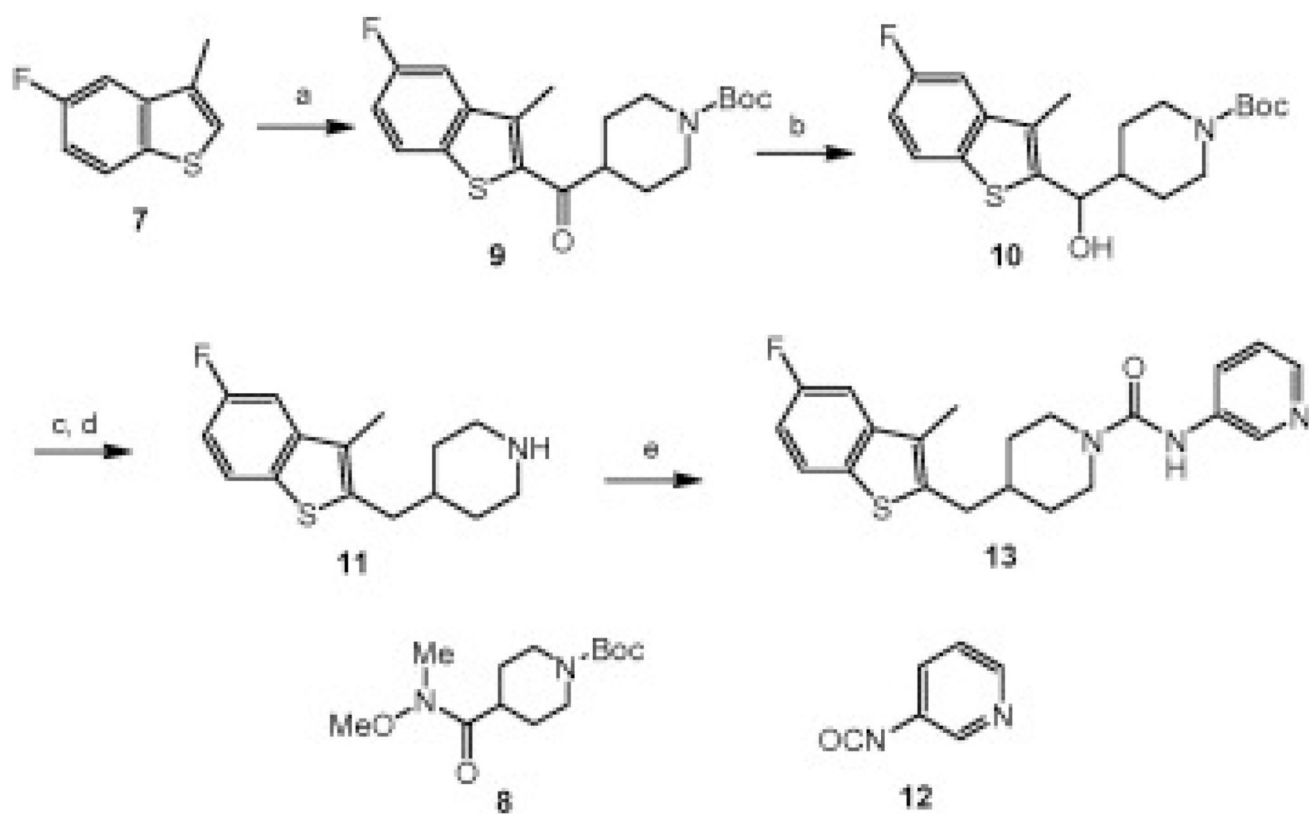


Figure 7.

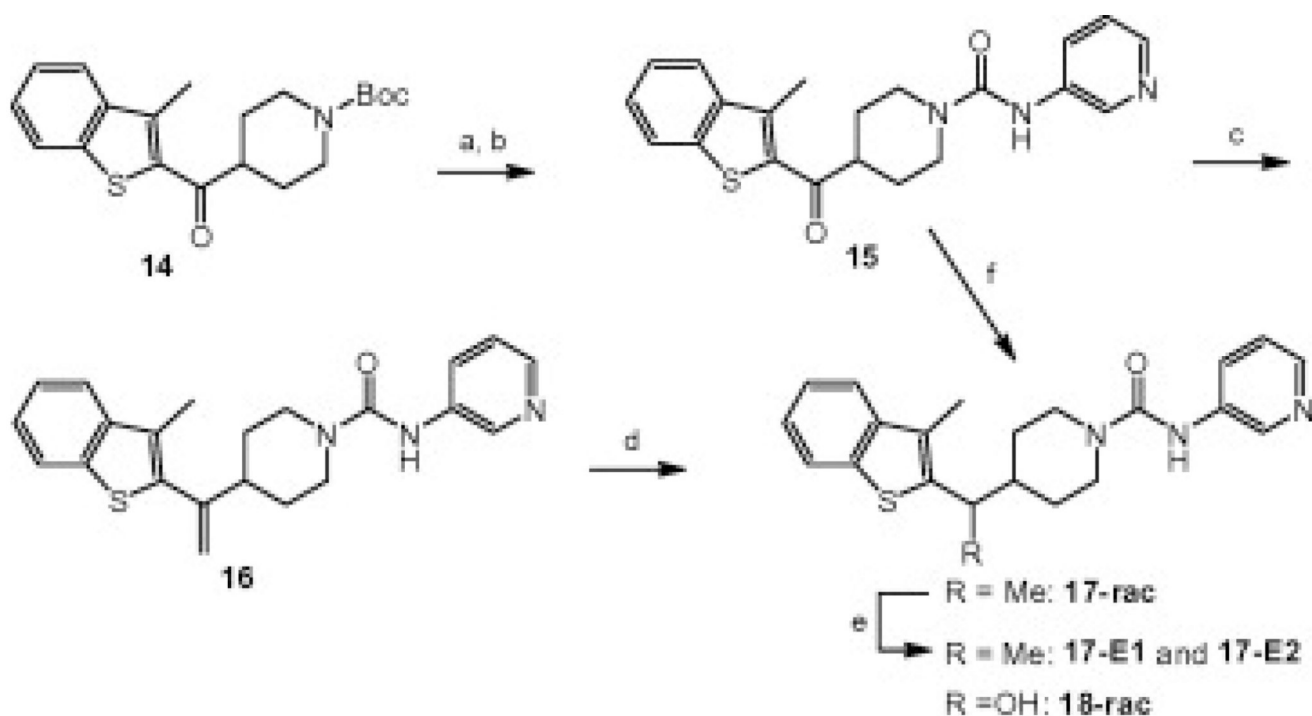
Anti-hyperalgesic effects of compound **6g** (3–30 mg/kg, ip) in the CFA model of inflammatory pain. Compound **6g** produces a dose-dependent reduction of mechanical allodynia (hyperalgesic) in rats (black bars). The effect of the non-steroidal anti-inflammatory drug naproxen (10 mg/kg, ip hatched bar) is shown for comparison. Anti-hyperalgesic responses were determined at 4 h following drug treatment and were significantly different between compound **6g**- and vehicle-treated groups ($p < 0.05$). $n = 8$ rats/group.

**Scheme 1.**

Synthesis of piperazine ureas **4** and **6**: (a) PhNCO, CH₂Cl₂, 92%; (b) TFA, CH₂Cl₂, 80–99% (c) NaBH(OAc)₃, DCE, 50–95%; (d) *N*-Boc-piperazine, NaBH(OAc)₃, CH₂Cl₂; then TFA, CH₂Cl₂, 64%; (e) RNCO (R = alkyl, Ph, 3-pyr; ie. **4d–g**, **4h**, **6a**), CH₂Cl₂, 50–90%; (f) RNHCO₂Ph (R = heterocycle, ie. **4j–l**, **6**), DMSO, 60 °C, 50–80%.

**Scheme 2.**

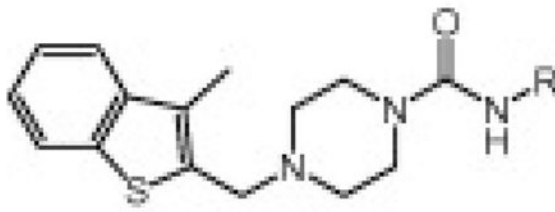
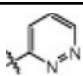

Synthesis of piperidine urea **13**: (a) *n*-BuLi, THF, $-78\text{ }^{\circ}\text{C}$; then add **8**, 70%, (b) NaBH_4 , EtOH, quant; (c) TsOH, toluene, quant; (d) $\text{H}_2(\text{g})$, 20% Pd/C, MeOH, 87%; (e) **12**, CH_2Cl_2 , 60%.

**Scheme 3.**

Synthesis of linker analogs **15–18**: (a) TFA, CH₂Cl₂, 99%; (b) **12**, CH₂Cl₂, 85%; (c) Ph₃PCH₃Br, *n*-BuLi, THF, –20 °C to rt, 97%; (d) H₂(g), Pd/C, MeOH, 76%; (e) chiral chromatography (CHIRALCEL[®] OD); (f) NaBH₄, EtOH, quant.

Table 1

Human and rat FAAH potency (k_{inact}/K_i values)¹⁵ for compounds **4a–l**, **6a** showing SAR of the right hand side of the urea

			
	R	hk_{inact}/K_i ($M^{-1} s^{-1}$)	rk_{inact}/K_i ($M^{-1} s^{-1}$)
4a	Butyl	44	13
4b	CH ₂ CH ₂ OH	42	<10
4c	CH ₂ C(O)NHMe	<10	<10
4d	<i>i</i> Pr	70	<10
4e	Cyclohexyl	<10	<10
4f	<i>t</i> Bu	<10	<10
4g	Bn	<10	<10
4h	Ph	1918	762
4i	2-pyr	1002	635
6a	3-pyr	2401	1083
4j		924	191
4k		1559	1433

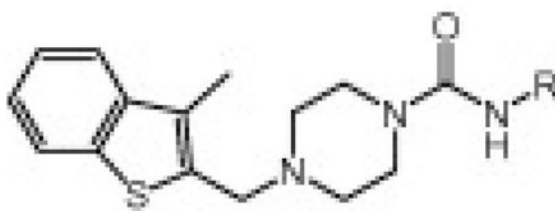
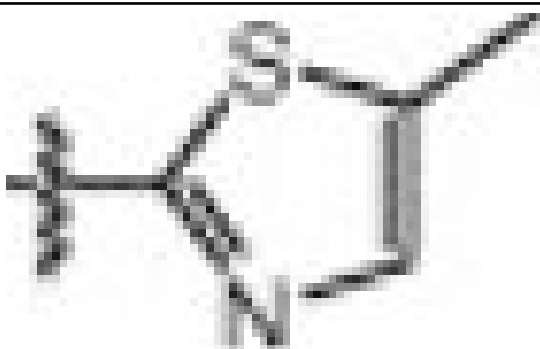
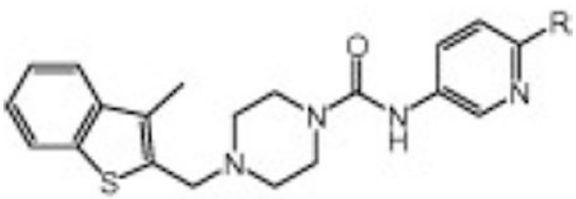
			
	R	hk_{inact}/K_i ($M^{-1} s^{-1}$)	rk_{inact}/K_i ($M^{-1} s^{-1}$)
4l		<10	<10

Table 2

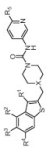
Human and rat FAAH potency (k_{inact}/K_i values)¹⁵ for compounds **6a–6n** showing SAR of substituted pyridyl ureas



	R	hk_{inact}/K_i ($M^{-1} s^{-1}$)	rk_{inact}/K_i ($M^{-1} s^{-1}$)
6a	H	2401	1083
6b	Me	1481	390
6c	CF ₃	69	<10
6d	Cl	1238	242
6e	Br	645	157
6f	Ph	631	1215
6g	OMe	2931	1060
6h	O-(3-Pyr)	605	101
6i	NH ₂	1871	1067
6j	NHMe	1108	1513
6k	NMe ₂	892	1811
6l	NHEt	597	1891
6m	NEt ₂	90	227
6n	NHAc	2011	1719

Table 3

Human and rat FAAH potency (k_{inact}/K_i values)¹⁵ for compounds **13**, **19–39** showing SAR of substituted benzothiothiophenes



	R ¹	R ²	R ³	R ⁴	R ⁵	X	hk_{inact}/K_i (M ⁻¹ s ⁻¹)	r_{k_{inact}/K_i} (M ⁻¹ s ⁻¹)
19	H	H	H	H	H	N	695	174
6a	Me	H	H	H	H	N	2401	1083
20	Me	H	H	H	H	C	5129	2613
21	Et	H	H	H	H	N	1402	774
22	Et	H	H	H	H	C	1668	1013
6b	Me	H	H	H	Me	N	1481	390
23	Cl	H	H	H	Me	N	900	133
24	Me	F	H	H	H	N	3321	1203
25	Me	F	H	H	H	C	4147	1547
26	Me	F	H	H	Me	N	1980	758
27	Me	H	F	H	H	N	3134	779
13	Me	H	F	H	H	C	4474	729
28	Me	H	Me	H	H	N	2635	557
29	Me	H	Me	H	H	C	3024	482
30	Me	H	Cl	H	H	N	2822	1133
31	Me	H	CF ₃	H	H	N	1389	219
32	Me	H	OMe	H	H	N	1381	500
33	Et	H	F	H	H	N	1808	617
34	Et	H	F	H	H	C	2292	1141
35	Me	H	F	H	Me	N	1871	260
36	Me	H	Me	H	Me	N	1169	183
37	Me	H	H	OMe	H	N	73	113
38	Me	H	H	OEt	H	N	14	<10
39	Cl	H	H	Me	Me	N	73	14

Table 4Human and rat FAAH potency (k_{inact}/K_i values)¹⁵ for compounds **15–18** showing SAR of the piperidine linker

	hk_{inact}/K_i ($\text{M}^{-1} \text{s}^{-1}$)	rk_{inact}/K_i ($\text{M}^{-1} \text{s}^{-1}$)
15	3601	1226
16	5441	991
17-rac	114	48
17-E1	34	<10
17-E2	617	110
18-rac	200	79